J. Biochem. **135**, 375–384 (2004)
DOI: 10.1093/jb/mvh045

Thermus thermophilus MutS2, a MutS Paralogue, Possesses an Endonuclease Activity Promoted by MutL

Kenji Fukui[2], Ryoji Masui[1,2] and Seiki Kuramitsu[*,1,2]

[1]Department of Biology, Graduate School of Science, Osaka University, 1-1 Machikaneyamacho, Toyonaka, Osaka 560-0043; and [2]RIKEN Harima Institute at SPring-8, 1-1-1 Kouto, Mikazuki-cho, Sayo, Hyogo 113-0033

Received November 13, 2003; accepted January 15, 2004

The mismatch repair system (MMR) recognizes and corrects mismatched or unpaired bases caused mainly by DNA polymerase, and contributes to the fidelity of DNA replication in living cells. In *Escherichia coli*, the MutHLS system is known to function in MMR, and homologues of MutS and MutL are widely conserved in almost all organisms. However, the MutH endonuclease has not been found in the majority of organisms. Such organisms, including *Thermus thermophilus* HB8, often possess the so-called MutS2 protein, which is highly homologous to MutS but contains an extra C-terminal stretch. To elucidate the function of MutS2, we overexpressed and purified *T. thermophilus* MutS2 (ttMutS2). ttMutS2 demonstrated the ability to bind double-stranded (ds) DNA, but, unlike ttMutS, ttMutS2 showed no specificity for mismatched duplexes. ttMutS2 ATPase activity was also detected and was stimulated by dsDNA. Our results also showed that ttMutS2 incises dsDNA. ttMutS2 incises not only oligo dsDNA but also plasmid DNA, suggesting that ttMutS2 possesses an endonuclease activity. At low concentrations, the incision activity was not retained, but was promoted by *T. thermophilus* MutL.

Key words: DNA repair, mismatch, MutS2, small MutS-related domain, *Thermus thermophilus*.

Abbreviations: MMR, mismatch repair; ttMutS2, *T. thermophilus* MutS2; dsDNA, double-stranded DNA; ttMutS, *T. thermophilus* MutS; ttMutL, *T. thermophilus* MutL; TLC, thin-layer chromatography; DTT, dithiothreitol; ssDNA, single-stranded DNA; MBP-ttMutL, maltose-binding protein-fused ttMutL; TAQ, *T. aquaticus*; aa, amino acid.

In living cells, a great amount of DNA damage arises as a result of errors during DNA replication, genetic recombination, and other processes (*1*, *2*). The accumulation of this damage can result in various genetic diseases. Many DNA repair systems have evolved to remove these lesions. One of them is the mismatch repair system (MMR), which is conserved throughout all organisms. In *Escherichia coli*, the early reactions of MMR are performed by the MutHLS system, which consists of three proteins, MutS, MutL and MutH (*3*). In this system, a mismatched base in the double-stranded (ds) DNA is recognized by a MutS dimer. A MutL dimer interacts with and stabilizes the MutS-mismatch complex, and then the MutH endonuclease is activated by MutL. MutH recognizes hemi-methylated GATC sites and then nicks the newly synthesized strand containing the error. To complete the repair, the strand containing the error is removed by an exonuclease and a new strand is synthesized by DNA polymerase. Homologues of *E. coli* MutS and MutL exist in many organisms ranging from bacteria to human, suggesting that the MutHLS system is common among those species (*4*, *5*). Interestingly, despite the prevalence of the MMR system, no homologue of *E. coli* MutH has been identified in the majority of organisms (*6*). MutH is a kind of restriction enzyme that functions in coordination with Dam methyltransferase, similar to a restriction-modification model. It is thought that this pair of enzymes originated in a single genome, moved to a few others, and was recruited to the MMR (*7*). This hypothesis might explain the observation that the majority of organisms does not possess these enzymes. Therefore, in organisms lacking *mutH*, MMR is not perfectly understood, and searches have been conducted for a new endonuclease involved in MMR.

As many genomes came to be deciphered, it became clear that many bacterial genomes lacking the *mutH* gene encode a MutS paralogue, MutS2, whose amino acid sequence is highly homologous to MutS. The term MutS2 was employed by Eisen (*6*) to represent *E. coli* MutS orthologues, which are not expected to be involved in MMR. He proposed that the MutS family can be classified into two distinct subgroups, MutS-I and MutS-II. MutS-I includes bacterial MutS, and eukaryotic MSH1-3 and MSH6, which are involved in MMR. MutS-II includes eukaryotic MSH4-5 and bacterial MutS2, which may be involved in crossing-over and chromosome segregation. With the exception of archaeal MutS2, MutS2 proteins contain an extra C-terminal region that does not exist in MutS and is called the small MutS-related (Smr) domain (*8*). Recently, Malik and Henikoff (*9*) proposed that the Smr domain has an endonuclease activity and that MutS2-like proteins are involved in MutL-independent MMR or meiotic chromosome crossing-over. However, there is currently no experimental evidence that clarifies the possible endonuclease activity of MutS2 proteins or

[*]To whom correspondence should be addressed at: Dept. of Biology, Graduate School of Science, Osaka University, Tel: +81-06-6850-5433, Fax: +81-06-6850-5442, E-mail: kuramitu@bio.sci.osaka-u.ac.jp

their Smr domain. In addition, genetic analyses suggested that *B. subtilis yshD*, a *mutS2* homologue, is expressed during the entire life cycle but not involved in recombinational events or post-replication mismatch repair (*10*). At present, the function of MutS2 is still unknown.

The *Thermus thermophilus* HB8 genome project (*11*) revealed the existence of not only MutS (ttMutS) and MutL (ttMutL), but also MutS2 (ttMutS2). Our laboratory has studied the functions and characteristics of ttMutS (*12–15*). Here we report the purification of ttMutS2 and characterization of its properties and activities, including evidence that ttMutS2 has the ability to incise a DNA strand.

EXPERIMENTAL PROCEDURES

MutS2 Gene Analysis—The *T. thermophilus* HB8 genome project revealed that the genome contains not only the tt*mutS* and tt*mutL* genes, but also a *mutS* paralogue, called tt*mutS2* (DDBJ/EMBL/GenBank accession No. AB107662; project code 0723). We compared the ttMutS2 sequence with the ttMutS sequence using the CLUSTAL W program and searched for homologues using the entire ttMutS2 sequence as a query for a BLAST search at NCBI (http://www3.ncbi.nim.nih.gov/cgi-bin/BLAST/). We also searched for homologues using the sequence of the C-terminal region of ttMutS2 (the C-terminal 100 residues), the Smr domain, as a query for a PSI-BLAST search (http://www3.ncbi.nlm.nih.gov/cgi-bin/BLAST/nph-psi_blast).

Plasmid Construction—Preliminary sequence data for the tt*mutS2* gene were provided by the *T. thermophilus* HB8 genome project. The tt*mutS2* gene was amplified from the genomic DNA by PCR. The forward and reverse primers were 5′-ATATCATATGATGCGTGACGTCCTC-GAGGTCCTGGAGTTC-3′ and 5′-ATATAGATCTTTAT-TATCAAAGCCGAAGCGCCACCACGGTAACCCC-3′, respectively (the underlines indicate the *Nde*I and *Bgl*II sites, respectively). The amplified fragment was ligated into the pT7Blue vector (Novagen). Sequence analysis revealed that the construction was error-free. The tt*mutS2* gene was then digested with the restriction enzymes *Nde*I and *Bgl*II and ligated into the compatible sites of the expression vector pET-11a (Novagen), creating the plasmid pET11a/ttmutS2 under control of the T7 promoter. The pET3a/ttmutS plasmid under control of the T7 promoter was constructed as described previously (*15*). The expression plasmid pMAL-cRI/ttmutL was a generous gift from Shiba. Briefly, the tt*mutL* gene is located downstream of the tt*mutS* gene, and it was previously cloned together with tt*mutS* by screening the ttHB8 cosmid library. The identified tt*mutL* gene was cloned into the vector pMAL-cRI (New England Biolab) to create the plasmid pMAL-cRI/ttmutL under control of the *tac* promoter. Details of the construction will be published elsewhere.

Overproduction and Purification of ttMutS2, ttMutS and MBP-ttMutL—E. coli BL21(DE3) (Novagen) was transformed with pET11a/ttmutS2 and grown at 37°C in 1.5 l YT medium containing 50 μg/ml ampicillin. When the density of cultures reached 4×10^8 cells/ml, isopropyl-β-D(−)-thiogalactopyranoside was added to 0.4 μM. Cells were grown at 37°C for 6 h after induction and harvested by centrifugation. Cells were lysed by sonication in buffer I (50 mM Tris-HCl, 5 mM β-mercaptoethanol, 1 mM EDTA, and 25% sucrose, pH 7.5) and treated at 70°C for 10 min. After centrifugation at 48,000 ×*g* for 60 min, the supernatant was loaded onto a phospho-cellulose column (bed volume 50 ml) equilibrated with buffer II (50 mM Tris-HCl, 5 mM β-mercaptoethanol, 1 mM EDTA, and 10% glycerol, pH 7.5). The column was washed with buffer II and eluted with a 500 ml gradient of 0–1,000 mM NaCl in buffer II. The fractions containing ttMutS2 were detected by SDS-PAGE, and ammonium sulfate was added to the fractions to yield a final concentration of 15% saturation. This solution was loaded onto a Toyopearl-phenyl column (bed volume 50 ml) equilibrated with buffer II containing 15% ammonium sulfate. The column was washed with 100 ml of the same buffer and eluted with a 500 ml gradient of 15–0% ammonium sulfate in buffer II. N-terminal sequencing of the purified protein confirmed it to be ttMutS2. ttMutS2 solution was stored at 4°C.

Maltose-binding protein-fused ttMutL (MBP-ttMutL) was overexpressed and purified according to the protocol established by Shiba. *E. coli* DH5α was transformed with pMAL-cRI/ttmutL and grown at 37°C in 1.5 l YT medium for 12 h. Harvested cells were disrupted by sonication in buffer III (50 mM Tris-HCl, 500 mM NaCl, 1 mM EDTA, 5 mM b-mercaptoethanol, and 10% glycerol, pH 8.0), and the cell lysate was centrifuged (48, 000 ×*g*) for 60 min. The supernatant was loaded onto an amylose resin column (bed volume 10 ml) equilibrated with buffer III. The column was washed with 50 ml of the same buffer and eluted with 50 ml of buffer IV (50 mM Tris-HCl, 1 mM EDTA, 5 mM b-mercaptoethanol, 10 mM maltose, and 10% glycerol, pH 8.0). The fractions containing MBP-ttMutL were further loaded onto a SuperQ column (bed volume 30 ml) equilibrated with 150 ml of buffer IV. The column was washed with 30 ml of buffer IV and eluted with a 200 ml gradient of 0–500 mM NaCl in buffer IV. Eluted MBP-ttMutL was stored at 4°C until use. ttMutS was prepared as described previously (*15*).

Size-Exclusion Chromatography—Size-exclusion chromatography was performed at 25°C using a Superdex 200 HR column (1 cm × 30 cm; Amersham Biosciences) in an AKTA system (Amersham Biosciences). A sample of 12 μM of ttMutS2 was eluted at a flow rate of 0.1 ml/min with a buffer containing 50 mM Tris-HCl (pH 7.5), 300 mM KCl and 10% glycerol. The column was calibrated using apoferritin (443,000), β-amylase (200,000), alcohol dehydrogenase (150,000), thyroglobulin (66,900), and cytochrome *c* (12,400). The elution profile was monitored by recording the absorbance at 280 nm.

ATPase Assay—The ATPase activity of ttMutS2 was assessed by thin-layer chromatography (TLC). The reaction mixture contained 0.5 μM ttMutS2, 1 μM [α-^{32}P]ATP, 1 mM ATP, 10 mM $MgCl_2$, 100 mM KCl, 1 mM dithiothreitol (DTT), and 50 mM Tris-HCl, pH 7.5, and incubated at 37 or 70°C for 45 min with or without 10 μM 37-bp double-stranded DNA (dsDNA), 5′-ATGTGAATCAGTATGG-TTCCTATCTGCTGAAGGAAAT-3′. Reactions were stopped by addition of equal volume of 50 mM EDTA. The samples were spotted on PEI cellulose sheets and eluted with TLC buffer (1 M formic acid and 0.5 M LiCl) for 60 min.

The sheets were dried and placed in contact with an imaging plate. The substrates and products were visualized and analyzed with a BAS2000 image analyzer (Fuji Photo Film).

Gel Shift Assay—Synthesized 20-mer single-stranded DNA (ssDNA), 5′-ATGTGAATCXGTATGGTTTC-3′, was radiolabeled at the 5′-end with [γ-^{32}P]ATP using polynucleotide kinase. The 5′-^{32}P-labeled ssDNA was annealed to the complementary ssDNA (5′-GAAACCATACYGATTCACAT-3′) to obtain dsDNA containing a matched or mismatched base pair (X = T for homoduplex, G-T mismatched heteroduplex and C-T mismatched heteroduplex; X = G for A-G mismatched heteroduplex; Y = A for homoduplex; Y = G for G-T mismatched heteroduplex; Y = C for C-T mismatched heteroduplex; and Y = A for A-G mismatched heteroduplex). The ^{32}P-labeled 20-bp dsDNA or 20-mer ssDNA substrates were incubated with ttMutS2 in 50 mM Tris-HCl, 100 mM KCl, 1 mM DTT, and 2 mM ATP, pH 7.5, for 30 min at 37°C. The mixture (10 μl) was loaded onto a 7.5% (w/v) polyacrylamide gel and electrophoresed in × 1 TBE buffer (89 mM Tris-borate and 2 mM EDTA). The gel was dried and placed in contact with an imaging plate. The bands were visualized and analyzed using a BAS2000 image analyzer.

Nuclease Assay Using Oligonucleotides—A 20-mer oligonucleotide, 5′-ATGTGAATCXGTATGGTTTC-3′, was synthesized, and its 5′ end was radiolabeled with [γ-^{32}P]ATP. This oligonucleotide was annealed to the oligonucleotide 5′-GAAACCATACYGATTCACAT-3′ to give matched or mismatched duplexes (X = T for homoduplex, G-T mismatched heteroduplex and C-T mismatched heteroduplex; X = G for A-G mismatched heteroduplex; Y = A for homoduplex; Y = G for G-T mismatched heteroduplex; Y = C for C-T mismatched heteroduplex; and Y = A for A-G mismatched heteroduplex). These duplexes were incubated with 0.5 μM ttMutS2 in a buffer containing 50 mM Tris-HCl, 100 mM KCl, 1 mM DTT, 2 mM $MgCl_2$, and 1 mM ATP, pH 7.5. Reactions were performed at 37°C for various periods and stopped by addition of an equal volume of sample buffer (5 mM EDTA, 80% deionized formamide, 10 mM NaOH, 0.1% bromophenol blue, and 0.1% xylene cyanol). The reaction mixtures were loaded onto 25% acrylamide gels (8 M urea and ×1 TBE buffer) and electrophoresed with × 1 TBE buffer. The gel was analyzed as described above. In the ttMutS2 dose-dependence experiment, the 30-bp duplexes were used, and k_{app}s were calculated on the basis of the amount of products at the appropriate reaction time for each concentration of ttMutS2. When the assay was carried out in the presence of MBP-ttMutL, its concentration was 250 nM.

The substrate ^{32}P-labeled DNA was base-specifically modified and digested according to the Maxam-Gilbert method (*16*). In order to determine the length of the product DNA, these fragments were mixed with sample buffer (1 mM EDTA, 80% deionized formamide, 10 mM NaOH, 0.1% bromophenol blue, and 0.1% xylene cyanol) and electrophoresed along with the products on DNA sequencing gels (25% acrylamide, ×1 TBE, and 8 M urea).

Nuclease Assay Using Plasmid DNA—The pT7Blue plasmid was electrophoresed and super-coiled DNA was collected by Recochip (Takara). The substrate super-coiled DNA (50 ng/μl) was incubated with ttMutS2 (1 μM) in 50 mM Tris-HCl, 100 mM KCl, 2 mM $MgCl_2$, 1 mM DTT, and 2 mM ATP, pH 7.5, at 70°C. The reaction was stopped by addition of ×5 loading buffer (5 mM EDTA, 50% glycerol, and 0.05% bromophenol blue), then loaded onto a 0.7% agarose S (Takara) gel containing ×0.5 TBE buffer and 10 mg/ml ethydium bromide and electrophoresed. The DNA fragments were stained with ethydium bromide and detected with UV light at 254 nm.

Detection of the Interaction Between MutS2 and MBP-ttMutL—A phospho-cellulose column (bed volume 1 ml) was equilibrated with a buffer (50 mM Tris-HCl, 5 mM DTT, 1 mM EDTA, 100 mM KCl, 5 mM ATP and 10% glycerol, pH 7.5), then 200 μl of 0 or 10 μM ttMutS2 in the same buffer was loaded onto the column. After washing with 1 ml of the same buffer, 200 μl of 10 μM MBP-ttMutL in the same buffer was loaded onto the column. Then, proteins were eluted with an 8 ml gradient of 0–500 mM KCl in the same buffer and detected by SDS-PAGE.

RESULTS

Sequence Comparison of ttMutS2, ttMutS and Other MutS Homologues—ttMutS is composed of 819 residues, while ttMutS2 has 744 residues (Fig. 1). Although these proteins share a highly homologous core region, ttMutS2 lacks residues 1–279 at the N-terminus of ttMutS and contains an extra stretch encompassing about 200 residues in the C-terminal region (544–744) that ttMutS does not have. The structural analysis of *Thermus aquaticus* (TAQ) MutS complexed with a heteroduplex DNA revealed that the N-terminal region of MutS contains the DNA-binding domain that is involved in recognition of a mismatched base (*17*). Interestingly, ttMutS2 lacks this region. According to Eisen's suggestion (*6*), the term MutS2 refers to a paralogue of MutS, which is not expected to be involved in mismatch-recognition. The structural analysis of TAQ MutS also revealed that the central and C-terminal regions of MutS contain the dsDNA-binding domain and the ATPase domain, respectively. The ATPase domain of MutS includes a Walker's A-type nucleotide-binding motif and also constitutes a dimerization domain. Dimerization is essential for formation of the nucleotide-binding site (*17*). Moreover, analysis of deletion mutants of the *E. coli mutS* gene revealed that the C-terminal ATPase domain is also required for MutS-MutL interaction (*18*). These regions are shared by ttMutS and ttMutS2.

It is likely that there are primarily three classes of MutS2: bacterial MutS2, archaeal MutS2 and plant MutS2 (Fig. 1). Bacterial MutS2 homologues were searched for using the entire ttMutS2 sequence as a query in a BLAST search. Archaeal and plant MutS2 homologues were searched for using the ttMutS2 ATPase and Smr domain sequences, respectively, as queries in a PSI-BLAST search. Bacterial MutS2, including ttMutS2, shares the homologous non-specific dsDNA-binding domain and the ATPase domain (dimerization domain) with TAQ MutS, and also contains the Smr domain. Similar architecture is also found in plant MutS2 from *Arabidopsis thaliana* and *Oryza sativa*. Unlike these proteins, archaeal MutS2 does not possess the Smr domain. Several bacteria, including *E. coli*, do not possess MutS2-like proteins; such species often have MutH and Dam methyl-

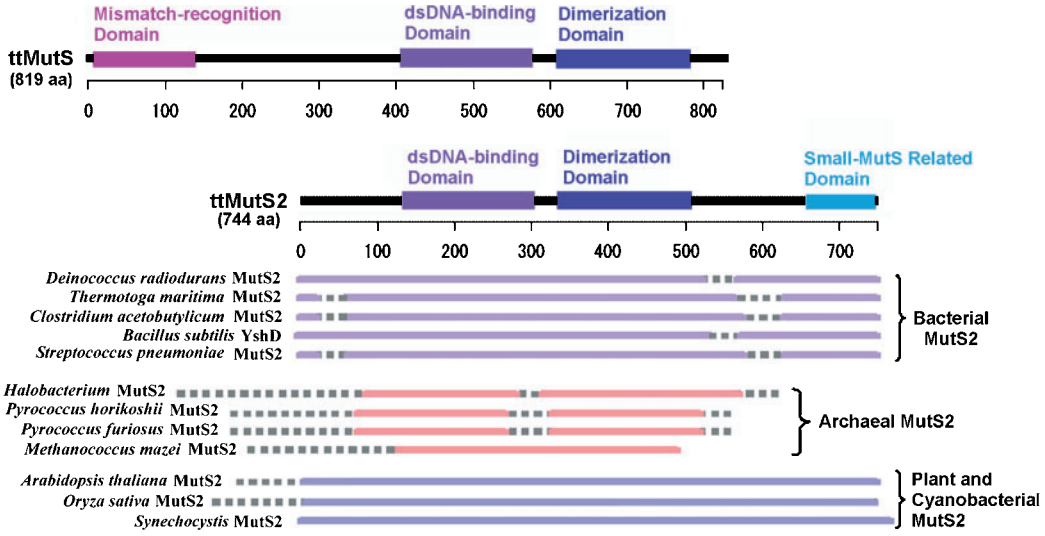

Fig. 1. **Schematic representation of sequence motifs in ttMutS and ttMutS2, and classification of the MutS2 lineage.** ttMutS entire sequence shows more than 90% identity to that of TAQ MutS, whose crystal structure has been solved (*17*). *dsDNA-binding Domain* and *ATPase Domain* of ttMutS2 indicate the regions that show more than 30% identity to the respective domains of TAQ MutS. *Smr domain* in ttMutS2 represents the region that shows about 30% identity to other bacterial Smr domains. Solid and broken lines indicate the regions with more than and less than 30% identity to the corresponding regions of ttMutS2, respectively. Bacterial MutS2 homologues were searched for using the entire ttMutS2 sequence as a query for a BLAST search. Archaeal and plant MutS2 homologues were searched for using the ttMutS2 ATPase and Smr domain sequences, respectively, as queries for PSI-BLAST searches. Homologous regions of these proteins were estimated from the sequence alignment made by the CLUSTAL W program. The accession numbers of the sequences are; NP295699 (*Deinococcus radiodurans* MutS2), NP229083 (*Thermotoga maritima* MutS2), NP348956 (*Clostridium acetobutylicum* MutS2), D69985 (*Bacillus subtilis* YshD), NP357962 (*Streptococcus pneumoniae* MutS2), NP279308 (*Halobacterium* sp. NRC-1 MutS2), NP142423 (*Pyrococcus horikoshii* MutS2), NP578203 (*Pyrococcus furiosus* MutS2), NP633398 (*Methanococcus mazei* Goe1 MutS2), CAE05741 (*Oryza sativa* MutS2), and P73625 (*Synechocystis* sp. PCC6803 MutS2).

transferase. It has been reported that an archaeal MutS2 from *Pyrococcus furiosus* was purified (*19*), but there has been no report describing the purification of a bacterial or plant MutS2. Here, we describe the purification and the characterization of bacterial MutS2 protein for the first time (see Experimental Procedures for details).

Overproduction and Purification of ttMutS2 and MBP-ttMutL—ttMutS2 was expressed in *E. coli* BL21 (DE3) under control of an IPTG-inducible T7 promoter. The induced band was observed at ~83 kDa (Fig. 2A), which corresponds to the molecular mass calculated from the amino acid sequence of ttMutS2. After removal of most of the endogenous *E. coli* proteins by heat treatment, the protein was purified to homogeneity by sequential column chromatography on phospho-cellulose and Toyopearl-phenyl (Fig. 2A). The N-terminal of amino acid sequence was found to be M-R-D-V-L-E-V-L-. The sequence was identical to that expected after translation from the nucleotide sequence of the tt*mutS2* gene.

ttMutL was overexpressed as an MBP-fused protein (~103 kDa). After column chromatography on amylose resin and SuperQ, the protein was purified to homogeneity (Fig. 2B).

Ability to Dimerize—According to the crystal structure of TAQ MutS homodimer complexed with a heteroduplex DNA, MutS is expected to bind to the substrate DNA as a dimer (*17*). Since ttMutS2 has a corresponding dimerization domain, we assessed the ability of ttMutS2 to form homodimers by using size-exclusion chromatography. As ttMutS2 easily aggregated, the experiment was performed with elution buffer containing 300 mM KCl, which efficiently prevented the aggregation. The majority of ttMutS2 at 10 μM eluted in the void volume of the column, but a small fraction of the protein eluted at a volume corresponding to an apparent molecular weight of 193,000 (Fig. 3). As the molecular mass of a ttMutS2 monomer is 82,500, this result suggests that some of the ttMutS2 forms homodimers in solution.

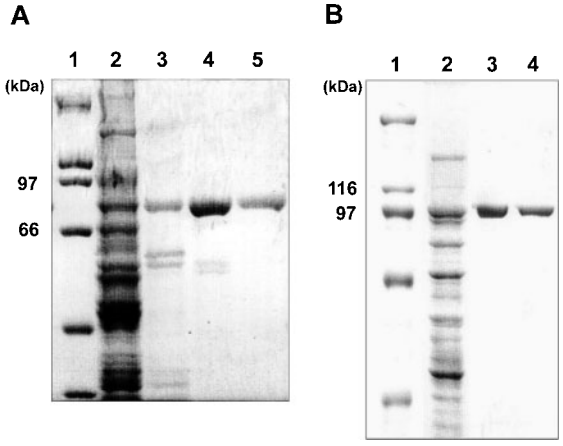

Fig. 2. **Overproduction and purification of ttMutS2 and MBP-ttMutL.** (A) Lane 1, molecular mass markers; lane 2, total cell extract; lane 3, supernatant after heat treatment; lanes 4 and 5, phospho-cellulose and Toyopearl-phenyl chromatography fractions, respectively. (B) Lane 1, molecular mass markers; lane 2, total cell extract; lanes 3 and 4, amylose resin and SuperQ chromatography fractions, respectively.

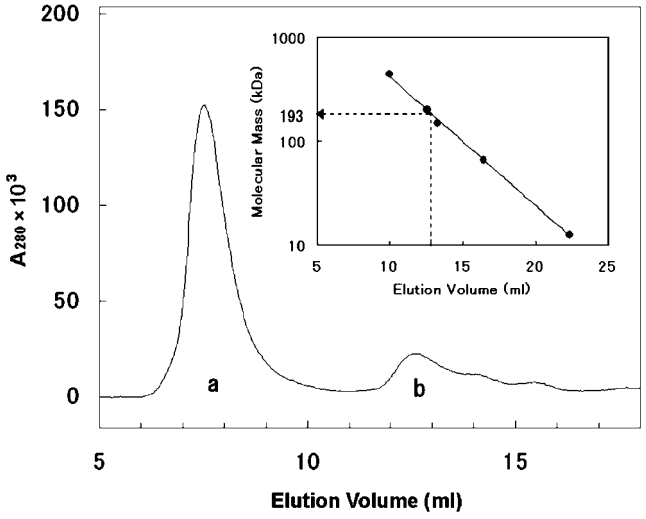

Fig. 3. **Size-exclusion chromatography.** Elution profile of 12 μM ttMutS2 on Superdex 200 HR. The apparent molecular mass of the peak (b) was estimated to be approximately 193,000, from the calibration curve shown in the inset. The elution volume of the peak (a) was the void volume of the column. Apoferritin (443,000), β-amylase (200,000), alcohol dehydrogenase (150,000), thyroglobulin (66,900) and cytochrome *c* (12,400) were used as molecular size markers.

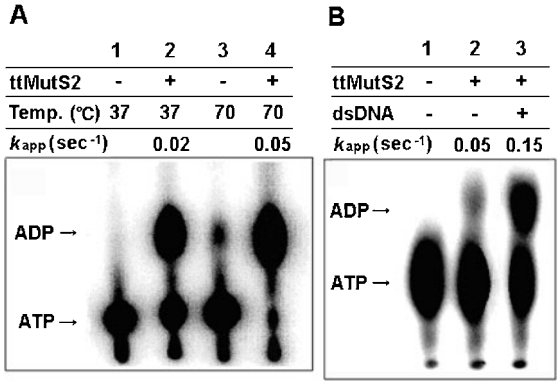

Fig. 4. **ATPase activity of ttMutS2.** (A) Lane 1, no protein at 37°C; lane 2, ttMutS at 37°C; lane 3, no protein at 70°C; lane 4, ttMutS2 at 70°C. (B) Effect of dsDNA. Lane 1, no protein or dsDNA at 70°C; lane 2, ttMutS2 without dsDNA at 70°C; lane 3, ttMutS2 with 37 bp dsDNA at 70°C.

ATPase Assay—ttMutS contains a Walker's A-type nucleotide-binding motif and shows weak ATPase activity (*15*). The ATPase domain is also the dimerization domain, and it is thought that dimerization of MutS is necessary to form the nucleotide-binding site. Since MutS2 possesses an ATPase domain homologous to that of MutS and size-exclusion chromatography verified the existence of a homodimeric form of ttMutS2, it was hypothesized that ttMutS2 might be able to hydrolyze ATP. Therefore, we used the TLC method to investigate the ability of ttMutS2 to hydrolyze ATP.

The measurements demonstrated that ttMutS2 has ATPase activity (Fig. 4). The activity at 70°C was higher than at 37°C, indicating that the hydrolysis was carried out by the thermostable ttMutS2 protein, not by other proteins from host cells. Figure 4B also shows that the

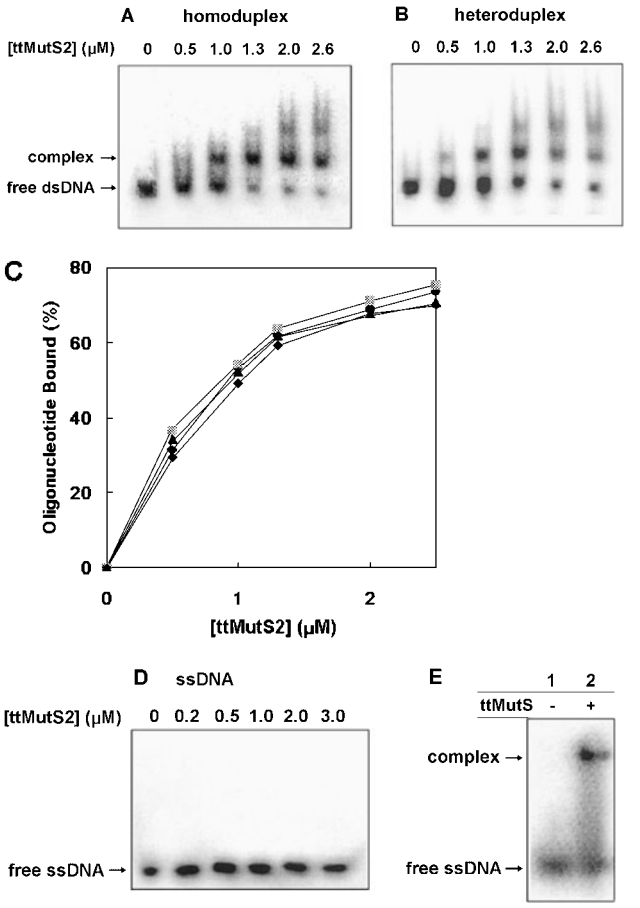

Fig. 5. **DNA-binding ability of ttMutS2.** (A) 20-bp homoduplex. (B) 20-bp G-T mismatched heteroduplex. (C) Dependence of the amount of shifted bands on ttMutS2 concentration. Circles, homoduplex; squares, G-T mismatched heteroduplex; triangles, G-A mismatched heteroduplex; and diamonds, C-T mismatched heteroduplex. (D) 20-mer ssDNA with ttMutS2. (E) 20-mer ssDNA with ttMutS.

ATPase activity was activated by a dsDNA. This result suggests that ttMutS2 interacts with dsDNA. There was no difference between the extent of activation by homoduplex and G-T mismatched heteroduplex DNA (data not shown).

DNA-Binding Activity—Dimeric ttMutS binds with higher affinity to G-T mismatched heteroduplex DNA than to homoduplex DNA (*15*). ttMutS2 retains the dimerization domain and non-specific dsDNA-binding domain, but not the mismatch-recognition domain. In addition, the ATPase assay showed ttMutS2 might interact with dsDNA. To verify the ability of ttMutS2 to bind to DNA and determine whether it exhibits a preference for a mismatched duplex, binding to 20-bp dsDNA with or without a mismatched base at the center of the strand was examined by gel shift assay. As shown in Figs. 5, A and B, complexes of ttMutS2 with dsDNA were detected. However, ttMutS2 bound to homoduplex and heteroduplex DNA with equivalent affinity (Fig. 5C). It should be noted that supershifted bands were detected at higher concentrations of ttMutS2 with both substrates. These bands might represent the binding of the second mole-

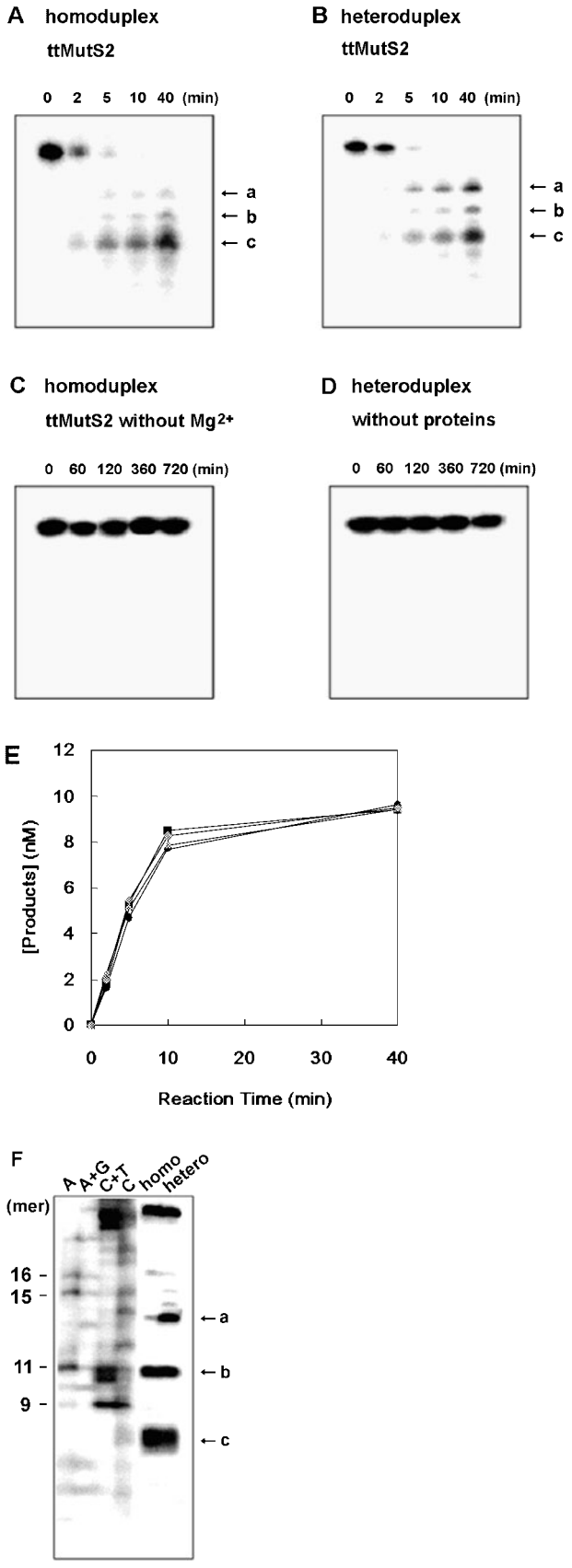

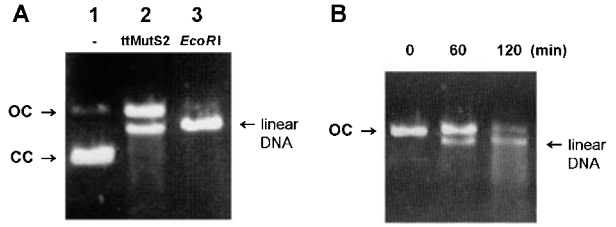

Fig. 7. **Nuclease activity for a plasmid DNA.** (A) Lane 1, without proteins; lane 2, with ttMutS2; and lane 3, with *Eco*RI. Arrows CC, OC and Linear DNA indicate the closed circular form and open circular form of the plasmid and linear dsDNA, respectively. (B) The DNA product indicated by arrow OC in A-lane 2 was recovered, and incubated with ttMutS2 under the same condition as A-lane2.

cule of ttMutS2 to the substrate dsDNA, or formation of ttMutS2 oligomers on the dsDNA.

Another difference between ttMutS2 and ttMutS was that ttMutS2 did not bind to ssDNA (Fig. 5D), whereas ttMutS did (Fig. 5E). This difference must arise from the N-terminal mismatch-recognition domain of ttMutS; the crystal structure of TAQ MutS (*17*) shows that recognition of mismatched bases is performed by recognition of ssDNA in the heteroduplex.

Nuclease Activity for Oligonucleotides—To verify the hypothesis that MutS2 possesses an endonuclease activity, 5′-end-labeled 20-bp oligonucleotides were incubated with ttMutS2. When the reaction mixture was separated by gel electrophoresis, several discrete radioactive bands were observed (Fig. 6, A and B). Control lysate from cells transformed with the pET-11a plasmid had no nuclease activity (data not shown). In addition, non-enzymatic degradation was not observed (Fig. 6D). Therefore, these results indicate that ttMutS2 has nuclease activity.

There was no significant difference in the digestion pattern or the intensity of the activity between homoduplex and heteroduplex DNA (Fig. 6, A, B and E). Divalent cations were necessary for the nuclease activity of ttMutS2 (Fig. 6C), while dsDNA-binding activity did not require divalent cations (Fig. 5, A and B). Electrophoresis with a DNA size marker indicated that the three main products, indicated by a, b and c, were 8-, 11- and 14-mers, respectively (Fig. 6F).

Nuclease Activity for Plasmid DNA—To determine whether ttMutS2 possesses an endonuclease activity, super-coiled plasmid DNA was incubated with ttMutS2 (Fig. 7A, lane 2). In comparison with lane 1 (closed circular plasmid alone) and lane 3 (the plasmid cut at one site by *Eco*RI), the lower band in lane 2 was thought to be linear dsDNA, while the upper was open circular DNA.

Fig. 6. **Nuclease activity for oligonucleotides.** (A) 20-bp homoduplex. (B) 20-bp G-T mismatched heteroduplex. (C) 20-bp homoduplex in buffer without $MgCl_2$. (D) 20-bp homoduplex without proteins. (E) Time course of ttMutS2 nuclease activity using various substrates. The concentrations of all products were plotted against incubation time. Circles, homoduplex; squares, G-T mismatched heteroduplex; triangles, G-A mismatched heteroduplex; and diamonds, C-T mismatched heteroduplex. (F) Reaction mixtures of 20-bp homoduplex and heteroduplex were electrophoresed along with DNA size markers constructed by the Maxam-Gilbert method. Arrows a, b, and c correspond to the respective arrows in panels A and B.

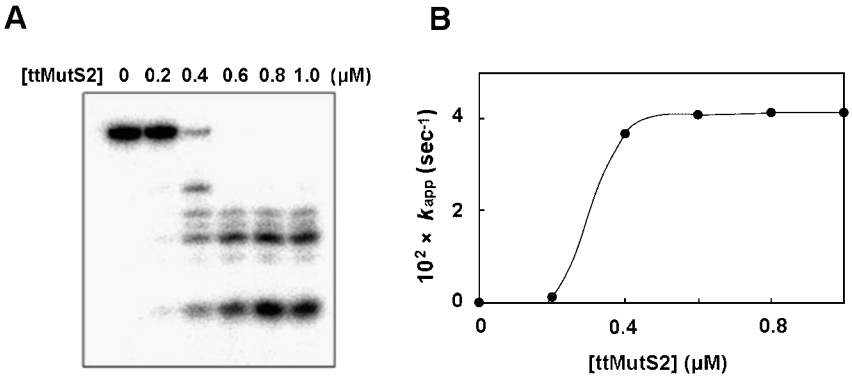

Fig. 8. **The effect of ttMutS2 concentration on nuclease activity.** (A) 30-bp heteroduplex was incubated with various concentrations of ttMutS2. Lanes 1–6, incubated for 120, 120, 10, 10, 5 and 5 min, respectively. These reaction times were selected to determine k_{app}s for each concentration of ttMutS2. (B) k_{app}s were determined and plotted against the concentrations of ttMutS2.

When the upper band was recovered and incubated again with ttMutS2, the large product was digested to the lower band, and further digestion resulted in the tailing of the lower band (Fig. 7B). These results strongly suggest that ttMutS2 possesses endonuclease activity. These reactions were performed at 70°C. Retention of activity at the higher temperature means that the digestion of plasmid DNA could be ascribed to protein from the thermostable organism and not from host cells. Moreover, the control experiment used in the former nuclease assay was applied here, and no digestion was observed (data not shown).

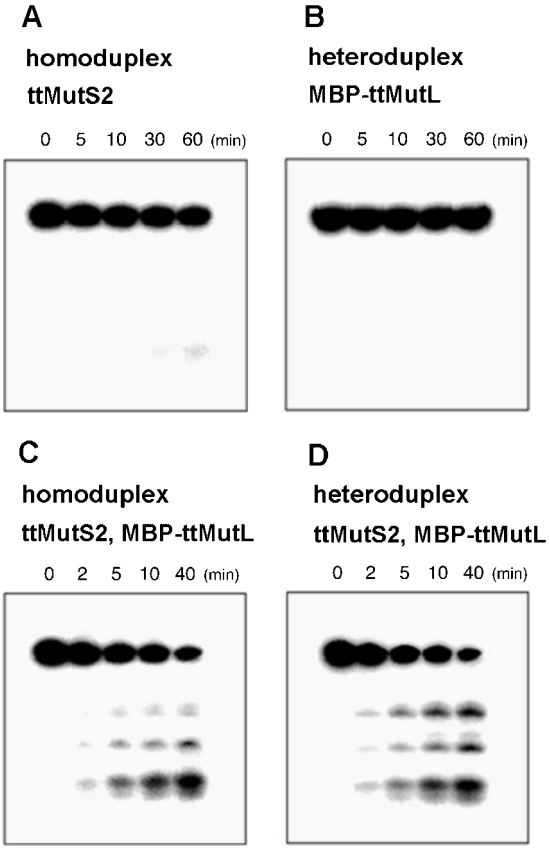

Fig. 9. **The effect of MBP-ttMutL on nuclease activity of ttMutS2.** (A) 20-bp G-T mismatched heteroduplex with ttMutS2. (B) 20-bp G-T mismatched heteroduplex with MBP-ttMutL. (C) 20-bp homoduplex with ttMutS2 and MBP-ttMutL. (D) 20-bp G-T mismatched heteroduplex with ttMutS2 and MBP-ttMutL.

ttMutS2 Nuclease Activity Was Promoted by MBP-ttMutL—We assessed the dependence of the nuclease activity on ttMutS2 concentration (Fig. 8A). The apparent velocity of the nuclease activity versus ttMutS2 concentration showed a sigmoidal response (Fig. 8B). This may be related to the dimeric state of ttMutS2, which is dependent on protein concentration.

E. coli MutL interacts with *E. coli* MutS on dsDNA (*20*), and deletion mutation analysis of the *E. coli mutS* gene revealed that the C-terminal region of MutS is essential for MutS-MutL interaction (*18*). Since ttMutS2 contains a region homologous to the C-terminal region of MutS (Fig. 1), a ttMutS2-ttMutL interaction was hypothesized. Therefore, we tested the effect of MBP-ttMutL on the activity of 100 nM ttMutS2, which cannot incise dsDNA. ^{32}P-labeled 20-bp homoduplex and G-T mismatched heteroduplex DNA were used as substrates. After incubation for various times, the reaction mixtures were electrophoresed on a denaturing gel and analyzed. While 100 nM ttMutS2 alone could not incise the substrates (Fig. 9A), the addition of MBP-ttMutL activated the nuclease activity (Fig. 9, C and D). As shown in Fig. 9B, MBP-ttMutL possessed no nuclease activity. Therefore, the digestion must have been carried out by ttMutS2 activated by MBP-ttMutL.

We tested whether ttMutS2 actually interacts with ttMutL by using a phospho-cellulose column. MBP-ttMutL did not bind to phospho-cellulose and eluted with a buffer containing no KCl (Fig. 10A). In the presence of ttMutS2, however, MBP-ttMutL was trapped in the col-

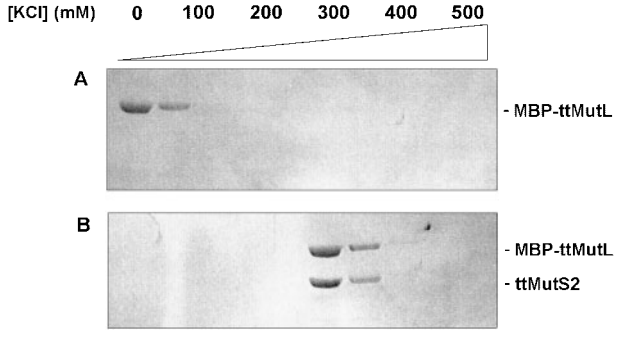

Fig. 10. **The interaction between ttMutS2 and MBP-ttMutL.** (A) 10 μM MBP-ttMutL was loaded onto a phospho-cellulose column in the absence of ttMutS2, and eluted with 0–500 mM KCl gradient. (B) The same experiment was carried out in the presence of ttMutS2.

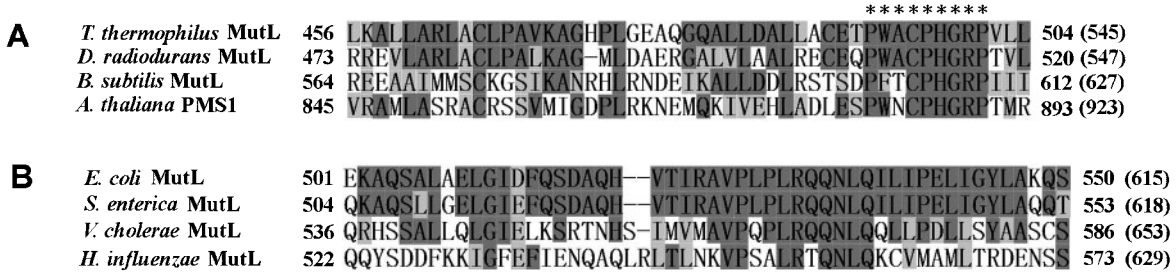

Fig. 11. **The sequence alignments of the C-terminal regions of MutL.** Numbers on the left and right indicate the distances from the protein N-termini. Numbers in the parentheses correspond to the full sequence size of the protein. Dark gray backgrounds indicate the perfect match of residues with that of ttMutL or *E. coli* MutL. Light gray backgrounds indicate residues whose chemical characteristics are conserved. (A) MutL from organisms which possess MutS2. The residues indicated by asterisks are well conserved not only among bacterial and plant MutL but also among eukaryotic MutL homologues. (B) MutL from organisms which possess MutH. The accession numbers of the sequences are BAA87903 (*T. thermophilus* MutL), NP295419 (*D. radiodurans*), NP389587 (*B. subtilis* MutL), AAL01156 (*A. thaliana* PMS1), NP418591 (*E. coli* MutL), NP458795 (*S. enterica* MutL), NP229999 (*V. cholerae* MutL) and NP438240 (*H. influenzae* MutL).

umn and did not elute until ttMutS2 eluted with a buffer containing about 300 mM KCl (Fig. 10B). Thyroglobulin (66.9 kDa) was used as a control and was not trapped in the column in the presence or absence of ttMutS2 (data not shown). These results indicate that ttMutS2 interacted with MBP-ttMutL. However, MBP-ttMutL did not introduce any change of the degradation pattern or specificity for mismatched heteroduplex (Fig. 9, C and D).

DISCUSSION

The most striking result of this study is the finding that ttMutS2 has a nuclease activity. To the best of our knowledge, this is the first report in which the nuclease activity of purified bacterial MutS2 has been experimentally verified. ttMutS2 digested oligonucleotides without specificity for mismatched bases (Fig. 6). When ttMutS2 digested 20-mer oligonucleotides, the three main products were 8-, 11- and 14-mers (Fig. 6F). This digestion by ttMutS2 did not generate "one base ladder" products. This result can be explained by either endonuclease or exonuclease activity. Endonuclease activity with a slight preference for a certain sequence would lead to the fragment pattern seen in Fig. 6. Alternatively, these fragments could be produced if ttMutS2 possesses an exonuclease activity that recognizes the terminus of the oligonucleotide and incises several nucleotides from the terminus. As shown in Fig. 7, ttMutS2 was able to digest closed circular plasmids lacking both 3′ and 5′ ends; therefore, ttMutS2 must possess at least an endonuclease activity. Further digestion of the open circular form of the plasmid suggests that ttMutS2 has a nicking endonuclease activity or has an exonuclease activity in addition to the endonuclease activity. In both cases, it is obvious that ttMutS2 alone nonspecifically incises the dsDNA regardless of the presence or absence of lesions.

We found that ttMutS2 does not retain this activity at concentrations below 100 nM (Fig. 8). However, at such low concentrations, ttMutS2 was activated by the addition of MBP-ttMutL (Fig. 9). The MutL-interface in the C-terminal region of MutS is conserved in ttMutS2, and MBP-ttMutL did not have a nuclease activity. Therefore,

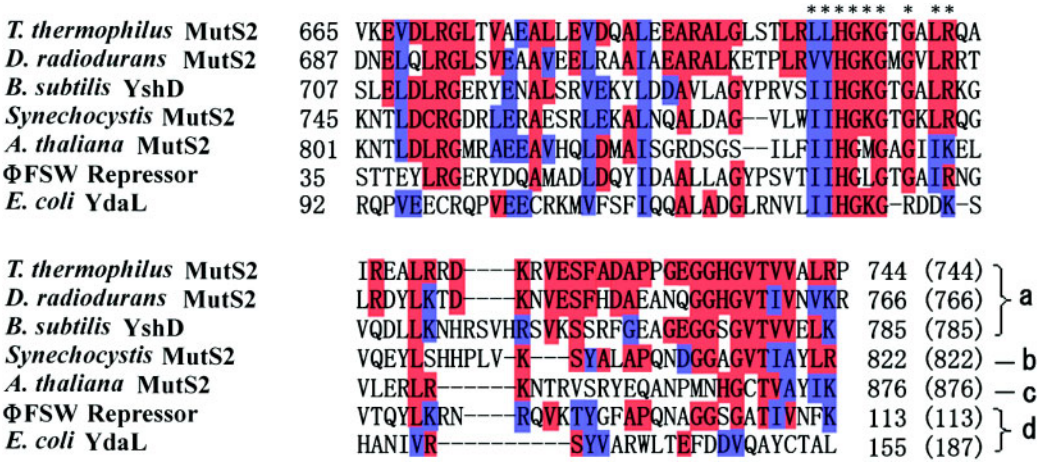

Fig. 12. **Sequence alignment of Smr domains.** Red backgrounds indicate the perfect match of residues with that of ttMutS2. Blue backgrounds indicate residues whose chemical characteristics are conserved. The residues indicated by asterisks show especially high conservation. (a) Bacterial Smr domains. (b) Cyanobacterial Smr domain. (c) Plant Smr domain. (d) Stand-alone Smr domains. The accession numbers of the sequences are indicated in the legend to Figure 1 except for AF406970 (*Lactobacillus casei* phage ϕFSW Repressor), and AAN80278 (*E. coli* YdaL).

it is reasonable to conclude that ttMutL activated ttMutS2. Furthermore, we detected the interaction between ttMutS2 and MBP-ttMutL using a phospho-cellulose column (Fig. 10). Bacterial and plant MutL most likely promote the dimerization of MutS2 on the dsDNA through direct interaction with MutS2.

In *E. coli*, MutL stimulates MutH endonuclease, and the C-terminal region of *E. coli* MutL is required for the activation of *E. coli* MutH (*21*). The C-terminal regions of MutL from organisms lacking MutH are relatively homologous to each other, but are not homologous to the C-terminus of *E. coli* MutL (Fig. 11). This raises the possibility that the C-terminal region of ttMutL interacts with the Smr domain of ttMutS2 instead of MutH. As it is expected that ttMutS2 has the MutL-interface, ttMutL might have two interaction sites for ttMutS2: the ttMutS interface and the Smr domain interface. The digestion patterns, however, were the same in the absence and presence of MBP-ttMutL, suggesting that even if ttMutL interacts with the Smr domain, it does not introduce any substrate specificity, and that other elements might restrict the cleavage site.

It is known that other nucleases are stimulated by MutL. *E. coli* MutH activity is stimulated by MutL in the absence of MutS and mismatched bases, and cleaves covalently closed circular DNA to generate nicked circular DNA (*21*). *E. coli* MutH does not digest nicked circular DNA to linear DNA fragments, since MutH recognizes the hemi-methylated GATC sequence in the substrate. Unlike MutH, ttMutS2 itself showed no substrate specificity, indicating that ttMutS2 is not merely a functional homologue of MutH. Even if ttMutS2 were involved in MMR in *T. thermophilus*, it would function *via* a different mechanism from *E. coli* MutHLS system. As for the MMR system, it has also been reported that a very-short-patch DNA repair protein, *E. coli* Vsr endonuclease, incises G-T mismatched heteroduplex DNA (*22*), and *E. coli* MutL stimulates binding of Vsr endonuclease to heteroduplex (*23*). Though *E. coli* Vsr endonuclease recognizes G-T mismatched base pairs and cleaves the phosphate backbone on the 5′ side of the thymine residue, ttMutS2 had no specificity for mismatched base pairs, suggesting that ttMutS2 is not a functional homologue of Vsr endonuclease. Thus, there are significant differences between ttMutS2 and other nucleases that are activated by MutL. In addition, only ttMutS2 is highly homologous to the MutS mismatch-recognition protein.

We have also determined that ttMutS2 has weak ability to form a homodimer, by size-exclusion chromatography (Fig. 3). MutS also possesses the ability to form a homodimer, and its dimerization domain has been identified (*17*, *24*). Comparison of ttMutS2 and ttMutS showed that ttMutS2 contains a region corresponding to the dimerization domain of MutS. Since the common dimerization domain exists in both ttMutS and ttMutS2, it may be possible for ttMutS2 to form the heterodimer with ttMutS. Moreover, the crystal structure of MutS dimer bound to a substrate DNA is asymmetric, and only one of the two molecules is involved in recognition of the mismatched or unpaired base (*17*, *24*). Thus, although MutS binds to dsDNA as a homodimer, it is heterodimeric in the aspect of function. We cannot exclude the possibility that a ttMutS2-ttMutS heterodimer recognizes a mismatched or unpaired base. The *T. thermophilus* HB8 genome project has determined that ttMutS and ttMutL are encoded in the same operon. Therefore, it is expected that ttMutS and ttMutL are expressed at the same time and regulate ttMutS2 cooperatively. Such cooperation between ttMutS and ttMutS2 might be analogous to the eukaryotic MMR, in which heterodimeric MutS homologues are known to function in MMR or recombinational events. In addition, it should be mentioned that no endonuclease has been identified for the eukaryotic MMR. MED1, the human methyl-CpG-binding endonuclease, was once thought to be a molecular determinant of strand-discrimination, like *E. coli* MutH, in eukaryotic MMR (*25*). However, current studies seem to rule out this possibility (*26*, *27*).

We assessed the ATPase activity of ttMutS2 (Fig. 4), which was stimulated by dsDNA. This result is consistent with our proposal that ttMutS2 binds to dsDNA as a dimer to generate an ATPase domain. However, the purpose for which ttMutS2 might utilize the energy of ATP hydrolysis is unknown. ATP hydrolysis might be related to the dynamics of dimerization or interaction with other proteins or DNA.

As illustrated in Fig. 1, MutS2 appears to be divided into three subgroups: bacterial MutS2, archaeal MutS2 and plant MutS2. Since archaeal MutS2 including *P. furiosus* MutS2 (*19*) does not possess the Smr domain, it might play a different role from bacterial MutS2. Interestingly, bacteria MutS2l and plant MutS2 are relatively similar to each other, especially in the presence of the Smr domain. Among the bacterial MutS2 proteins, cyanobacterial MutS2 is more homologous to plant MutS2 than others. This may reflect a phylogenetic relationship between cyanobacteria and plants. These conservations of MutS2 might be evidence that MutS2 plays an important role *in vivo* and that the Smr domain might contain a novel motif, as has been suggested by Malik and Henikoff (*9*). The sequence alignment of the Smr domain in Fig. 9 shows that not only MutS2 but another protein, *Lactobacillus casei* phage ϕFSW repressor protein (*28*), contains the Smr sequence. Moreira and Philippe (*8*) also reported that the Smr sequence is widely conserved in various organisms ranging from viruses to eukaryotes. These facts suggest that the Smr domain is a functional domain with a certain activity. Interestingly, the Smr domain contains a highly conserved histidine and two glycine residues in the center of the sequence, indicated by asterisks in Fig. 12. Histidine residues are able to function as catalytic residues of nucleases. For example, *E. coli* Vsr endonuclease, a site-specific endonuclease, possesses a catalytic histidine residue (*29*, *30*). If the Smr domain possesses nuclease activity, the histidine residue might be involved in this activity.

This study has demonstrated that ttMutS2 has an endonuclease activity that is promoted by MBP-ttMutL, suggesting that ttMutS2 might be involved in some kind of DNA repair reaction or recombinational events. MutS2 is defined as a bacterial MutS paralogue, which lacks the mismatch-recognition domain and is not expected to function in MMR (*6*). However, considering the possibility of heterodimerization of MutS2 with MutS and that mismatch recognition by MutS dimers is carried out by

only one of the two molecules, we suspect either the existence of an MMR pathway different from that in *E. coli*, or the existence of another DNA repair system. Rossolillo and Albertini (*10*) have reported that *B. subtilis* YshD, a ttMutS2 homologue, is not involved in post-replication mismatch repair; however, they did not rule out the participation of YshD in the repair of DNA damages different from those recognized by prokaryotic MutHLS system. Further experiments are required to determine whether MutS2 is engaged in MMR, another DNA repair system, or another pathway altogether.

This work was supported in part by Grants-in-aid for Scientific Research from the Ministry of Education, Science, Sports and Culture of Japan 13033025 (to S.K.) and 15570114 (to R.M.) Note: nucleotide sequence data reported are available in the DDBJ/EMBL/GenBank data bases under the accession number AB107661.

REFERECES

1. Friedberg, E.C., Walker, G.C., and Siede, W. (1995) DNA Damage. *DNA Repair and Mutagenesis*, pp. 1–58, American Society for Microbiology, N.W. Washington, D.C.
2. Worth, L., Clark, S., Radman, M., and Modrich, P. (1994) Mismatch repair proteins MutS and MutL inhibit RecA-catalyzed strand transfer between diverged DNAs. *Proc. Natl Acad. Sci. USA* **91**, 3238–3241
3. Modrich, P. (1989) Methyl-directed DNA mismatch correction. *J. Biol. Chem.* **264**, 6597–6600
4. Modrich, P. and Lahue, R. (1996) Mismatch repair in replication fidelity, genetic recombination, and cancer biology. *Annu. Rev. Biochem.* **65**, 101–133
5. Jiricny, J. (1998) Eukaryotic mismatch repair: an update. *Mutat. Res.* **409**, 107–121
6. Eisen, J.A. (1998) A phylogenomic study of the MutS family of proteins. *Nucleic Acids Res.* **26**, 4291–4300
7. Eisen, J.A. and Hanawalt, P.C. (1999) A phylogenomic study of DNA repair genes, proteins, and processes. *Mutat. Res.* **435**, 171–213
8. Moreira, D. and Philippe, H. (1999) Smr: a bacterial and eukaryotic homologue of the C-terminal region of the MutS2 family. *Trends Biochem. Sci.* **24**, 298–300
9. Malik, H.S. and Henikoff, S. (2000) Dual recognition-incision enzymes might be involved in mismatch repair and meiosis. *Trends Biochem. Sci.* **25**, 414–418
10. Rossolillo, P. and Albertini A.M. (2001) Functional analysis of the *Bacillus subtilis yshD* gene, a mutS paralogue. *Mol. Gen. Genet.* **264**, 809–818
11. Yokoyama, S., Hirota, H., Kigawa, T., Yabuki, T., Shirouzu, M., Terada, T., Ito, Y., Matsuo, Y., Kuroda, Y., Nishimura, Y., Kyogoku, Y., Miki, K., Masui, R., and Kuramitsu, S. (2000) Structural genomics projects in Japan. *Nat. Struct. Biol.* **7**, 943–945
12. Kato, R., Kataoka, M., Kamikubo, H., and Kuramitsu, S. (2001) Direct observation of three conformations of MutS protein regulated by adenine nucleotides. *J. Mol. Biol.* **309**, 227–238
13. Tachiki, H., Kato, R., and Kuramitsu, S. (2000) DNA binding and protein-protein interaction sites in MutS, a mismatched DNA recognition protein from *Thermus thermophilus* HB8. *J. Biol. Chem.* **275**, 40703–40709
14. Tachiki, H., Kato, R., Masui, R., Hasegawa, K., Itakura, H., Fukuyama, K., and Kuramitsu, S. (1998) Domain organization and functional analysis of *Thermus thermophilus* MutS protein. *Nucleic Acids Res.* **26**, 4153–4159
15. Takamatsu, S., Kato, R., and Kuramitsu, S. (1996) Mismatch DNA recognition protein from an extremely thermophilic bacterium, *Thermus thermophilus* HB8. *Nucleic Acids Res.* **24**, 640–647
16. Gilbert, W. and Maxam, A. (1973) The nucleotide sequence of the *lac* operator. *Proc. Natl Acad. Sci. USA* **70**, 3581–3584
17. Obmolova, G., Ban, C., Hsieh, P., and Yang, W. (2000) Crystal structures of mismatch repair protein MutS and its complex with a substrate DNA. *Nature* **407**, 703–710
18. Wu, Te-H. and Marinus, M.G. (1999) Deletion mutation analysis of the *mutS* gene in *Escherichia coli*. *J. Biol. Chem.* **274**, 5948–5952
19. Vijayvargia, R. and Biswas, I. (2002) MutS2 family protein from *Pyrococcus furiosus*. *Curr. Microbiol.* **44**, 224–228
20. Schofield, M.J., Nayak, S., Scott, T.H., Du, C., and Hsieh, P. (2001) Interaction of *Escherichia coli* MutS and MutL at a DNA mismatch. *J. Biol. Chem.* **276**, 28291–28299
21. Hall, M.C. and Matson, W. (1999) The *Escherichia coli* MutL protein physically interacts with MutH and stimulates the MutH-associated endonuclease activity. *J. Biol. Chem.* **274**, 1306–1312
22. Gonzalez-Nicieza, R., Turner, D.P., and Connolly, B.A. (2001) DNA binding and cleavage selectivity of the *Escherichia coli* DNA G:T-mismatch endonuclease (vsr protein). *J. Mol. Biol.* **310**, 501–508
23. Drotschmann, K., Aronshtam, A., Fritz, H.J., and Marinus, M.G. (1998) The *Escherichia coli* MutL protein stimulates binding of Vsr and MutS to heteroduplex DNA. *Nucleic Acids Res.* **26**, 948–953
24. Lamers, M.H., Perrakis, A., Enzlin, H.J., Winterwerp, H.H.K., Wind, N., and Sixma, T.K. (2000) The crystal structure of DNA mismatch repair protein MutS binding to a G·T mismatch. *Nature* **407**, 711–717
25. Bellacosa, A., Cicchillitti, L., Schepis, F., Riccio, A., Yeung, A.T., Matsumoto, Y., Golemis, E.A., Genuardi, M., and Neri, G. (1999) MED1, a novel human methyl-CpG-binding endonuclease, interacts with DNA mismatch repair protein MLH1. *Proc. Natl Acad. Sci. USA* **96**, 3969–3974
26. Bellacosa, A. (2001) Role of MED1 (MBD4) Gene in DNA repair and human cancer. *J. Cell Physiol.* **187**, 137–144
27. Drummond, J.T. and Bellacosa, A. (2001) Human DNA mismatch repair *in vitro* operates independently of methylation status at CpG sites. *Nucleic Acids Res.* **29**, 2234–2243
28. Binishofer, B., Moll, I., Henrich, B., and Blasi, U. (2002) Inducible promoter-repressor system from the *Lactobacillus casei* phage ϕFSW. *Appl. Environ. Microbiol.* **68**, 4132–4135
29. Tsutakawa, S.E., Muto, T., Kawate, T., Jingami, H., Kunishima, N., Ariyoshi, M., Kohda, D., Nakagawa, M., and Morikawa, K. (1999) Crystallographic and functional studies of very short patch repair endonuclease. *Mol. Cell* **3**, 621–628
30. Tsutakawa, S.E., Jingami, H., and Morikawa, K. (1999) Recognition of a TG mismatch: the crystal structure of very short patch repair endonuclease in complex with a DNA duplex. *Cell* **99**, 615–623